COMPARISON OF GLENOHUMERAL CONTACT PRESSURES AND CONTACT AREA AFTER GLENOID RECONSTRUCTION WITH LATARJET OR DISTAL TIBIAL OSTEOCHONDRAL ALLOGRAFT

Sanjeev Bhatia, MD†; Geoffrey S. Van Thiel MD, MBA*†; Deepti Gupta, BS†;
Neil Ghodadra, MD†; Bernard R. Bach, Jr. MD†; Elizabeth Shewman PhD†;
Vincent M. Wang PhD†; Anthony A. Romeo, MD†; Nikhil N. Verma, MD†;
CDR Matthew T. Provencher MD MC USN‡

†Division of Sports Medicine, Department of Orthopaedic Surgery, Rush University Medical Center, Rush Medical College of Rush University, Chicago, IL

*Rockford Orthopedic Associates, Rockford, IL

‡Department of Orthopaedic Surgery, Naval Medical Center San Diego, San Diego, CA

Introduction:

Understanding and properly addressing irregularities in the osseous architecture of the glenohumeral joint are critical to the overall success of surgical treatment of glenohumeral instability.(1-3) Following a traumatic anterior shoulder dislocation event, a concomitant glenoid rim fracture or attritional bone injury may compromise the static restraints of the glenohumeral joint, further perpetuating shoulder instability. Loss of the glenoid's bony articular conformity significantly inhibit its ability to withstand shear stress.(4)

Recognizing glenoid bone loss as a potential cause for failure in glenohumeral instability surgery has been recently emphasized by various authors calling attention to this often underappreciated problem.(1, 2, 4-7) Principles of surgical management are guided by the extent of osseous injury to the glenoid, the surgeon's personal experience with specific reconstructive techniques, and patient specific factors such as work and athletic demands.(1) Both arthroscopic(4, 8-11) and open techniques(5, 12-14) have been described and there is a growing body of evidence to suggest that bony reconstruction of the glenoid is recommended if there is significant bone loss (usually >20-25%).(1, 15)

For patients with significant bone defects, several autologous bone-grafting procedures, including the Latarjet (and modified Bristow) procedure as well as the use of iliac crest bone graft, have been described.(7, 16-18) Although long-term studies have demonstrated that such techniques result in stable and functional shoulders, arthritis continues to remain a concern.(15, 19-21) It is postulated that a nonanatomic repair of the glenoid arc, an extra-articular nonanatomic repair of capsulolabral tissues, and a lack of chondral surface reconstitution may in part explain the high incidence of degenerative disease after coracoid transfer. In a recent study, Ghodadra and authors showed that glenohumeral contact pressure is optimally restored with flush positioning of iliac or coracoid bone graft. Coracoid grafts that were placed proud significantly increased peak pressures within the joint and altered joint loading patterns—a finding that further supports the rationale for finding anatomic means for reconstruction of a congruous glenohumeral joint.

Reconstruction of glenoid bone defects with distal tibial osteochondral allograft has recently been described as a technique for restoring the articular surface of the glenoid while providing for a customized, anatomic fit of bone graft and avoiding coracoid morbidity. Although this technique provides the theoretical benefit of improved joint congruity and decreased contact pressures, it is unclear whether the distal tibial graft truly reduces glenohumeral contact pressures and congruity in comparison with coracoid grafts.

The purpose of this study is to determine changes in the magnitude and location of contact pressure after (1) creation of 30% anterior glenoid defect and (2) subsequent glenoid bone augmentation procedures with flush placement of a Latarjet coracoid graft or a distal tibial osteochondral graft. It is hypothesized that bone augmentation with the distal tibial osteochondral graft in a flush position will best normalize articular contact pressures while also providing complete glenoid bone restoration.

Methods

Eight fresh-frozen human cadaver shoulders (5 right shoulders and 3 left shoulders) from donors with a mean age of 49 [range, 38-58 years] at the time of death were dissected free of all soft tissues except the labrum (**Figure 1**). Demographic characteristics of cadaveric shoulder specimens can be found in **Table 1**. The capsule was sharply excised to expose the humerus and osseous glenoid with the labrum. Prior to potting the scapula in a methylmethacrylate block, digital calipers were used to measure the anterior-posterior and superior-inferior diameters of the glenoid with the labrum attached; dimensions were taken based on viewing the glenoid *en face* as a clock with the superior portion of the glenoid equivalent to twelve o'clock. Diameters were measured from twelve o'clock to six o'clock and from three o'clock to nine o'clock. The height, width (thickness), and length of the corresponding coracoids were also recorded.

The scapula was then potted in epoxy cement with the glenoid positioned parallel to the floor with a gravity-level in order to ensure that the joint would experience compressive loads rather than shearing forces during testing. Two perpendicular 0.45-in (11.4mm) Kirschner wires were inserted through the glenoid neck from the six o'clock to the twelve o'clock position and from the three o'clock to the nine o'clock position. These served as reference points to divide the glenoid into four quadrants and to insure consistent positioning of the pressure sensor pads between trials.

The corresponding humeral shaft was also potted in epoxy cement that was positioned to fit in a custom designed fixture mounted on an MTS closed-loop servohydraulic testing machine (MTS Systems, Eden Prairie, Minnesota). Only 2 cm of the proximal part of the shaft was left exposed in order minimize diaphyseal bending moments and interference from the testing apparatus during abduction. To define the neutral axis, the bicipital groove was oriented anteriorly and the humerus was externally rotated 10 degrees with a goniometer, with no applied abduction or flexion.

A 0.1-mm-thick dynamic pressure-sensitive pad (Tekscan 5051 pad; Tekscan, Boston, Massachusetts), with a 56x56-mm matrix and a density of 62 sensels/cm^2, was precalibrated with loaded MTS machine weights similar in size to the average glenoid. Calibration was performed per the manufacturer's guidelines, applying loads of 20% and 80% of the maximum test load (440N) across the glenohumeral joint. The pressure pad was inserted between the humerus and glenoid, with the four quadrants marked on the pad for identical positioning during sequential trials.

Testing Conditions

The MTS machine was used to apply a compressive load of 440N. Using the Tekscan sensor; glenohumeral contact pressure, contact area, and peak forces were determined. A load of 440 N was chosen on the basis of prior work(21) and serves as an approximate maximal load for simulation of in vivo glenohumeral loading conditions during the range of motion of the shoulder during activities of daily living.(22) The testing sequence included four conditions: (1) intact

glenoid, (2) glenoid with 30% anterior bone defect of glenoid surface area from two o'clock to six o'clock, (3) 30% glenoid defect with a Latarjet bone block placed flush with the lateral surface of the coracoid becoming the glenoid face (Latarjet-LAT), (4) 30% glenoid defect with a distal tibia bone block placed flush. An example of a specimen in each of these 4 states is depicted in **Figure 2**.

The following positions were tested for each condition: (1) 30° humeral abduction with a 440-N load, (2) 60° humeral abduction with a 440-N load, and (3) 60° humeral abduction and 90° humeral external rotation (ABER) with a 440-N load.

After each measurement, the pressure sensor was removed and then repositioned according to the previously placed quadrant marks. A new Tekscan sensor was utilized for each specimen, as our pretesting of Tekscan sensors showed a decrease in sensitivity and the ability to detect contact pressure after approximately 95 consecutive loads of 440N. Testing sensors utilized were thus well below the threshold of any potential decrease in sensitivity due to potential creep from repeated testing and handling of the sensor.

Bone Defects

An osteotomy simulating at least 30% bone loss was performed based on a modification of the glenoid bone loss quantification techniques put forth by Sugaya(11) and Burkhart(23). As noted in the literature, the amount of glenoid bone loss can be calculated by using the formula *Defect size = (B-A)/2B x 100%*, where *B* is the radius of the glenoid's true fit circle and *A* is the distance from the circle center to the edge of the defect (**Figure 3**). Because defect size was known (in our case, 30%), the formula was rearranged to algebraically solve for *A*. For each specimen, the anterior-posterior diameter of the glenoid (two times the radius, *B*) was precisely measured using digital calipers. The distance from the circle center to the osteotomy site (*A*) was then solved for algebraically. A true-fit circular template was then created with the same diameter as the glenoid specimen and was cut *A* millimeters from the center in order to replicate the 30% osteotomy site. The template was then applied to the glenoid and oriented such that a clinically relevant osteotomy, one parallel to the long axis of the glenoid, could be created. This orientation of the glenoid osteotomy is different from some prior cadaveric studies(22) but is more consistent with clinical bone loss.(11, 24, 25) Each glenoid osteotomy was made with the use of a 10x0.5mm sagittal saw set to 15,000 revolutions per minute to minimize bone loss. The template remained in place after each osteotomy to ensure that at least 30% of bone had been removed from the inferior portion of the glenoid. Mean glenoid defect width was 9.2±0.75mm (Range 8-10.5mm). Prior to testing, the new anterior-posterior diameter of the glenoid was measured in line with the glenoid bare spot. After each osteotomy, the testing sequence was repeated from neutral to the ABER position, with pressure sensor measurements recorded as described above.

Bone Augmentation Procedures

After the specimen was osteotomized to create a 30% anterior glenoid bone loss model, each of the eight cadaver specimens was randomly assigned to first undergo either a Latarjet-LAT autograft procedure, or a distal tibia bone graft procedure. For the Latarjet procedure, a mean of 29mm of the length of the coracoid process was harvested from the cadaver specimen's coracoid tip to the elbow of the coracoid base. Soft tissue attachments were sharply excised and the graft's width was recorded. The coracoid graft was rotated 90° such that the lateral aspect of the coracoid reconstituted the glenoid face and the inferior surface of the coracoid was apposed to the glenoid neck (**Figure 4**).(16, 26) Additionally, the graft was positioned so that the lateral surface was flush with the glenoid face.(21) Prior to fixation, the inferior surface of the coracoid was gently decorticated with the 0.5mm sagittal saw to replicate the clinical practice of denuding cortical bone on a bone graft for improved healing and incorporation into the glenoid. Two 1.6mm Kirschner wires, drilled in non-parallel fashion, were utilized to affix the bone block in place (Figure 4c). A reduction clamp (Synthes, West Chester, PA) was used to provide further compression across the construct and prevent subtle changes in position.

In order to perform glenoid augmentation with distal tibial osteochondral allograft, 8 distal tibial allografts (Allosource, Denver, CO) with a mean age of 19.8 ± 3.1 years (range 16-25) were procured. For each glenoid, a distal tibial allograft of the same laterality was utilized: e.g. right tibias were used for right glenoids and vice versa. As described by Provencher(12), an osteochondral distal tibial graft with the same dimensions as the glenoid defect was carefully cut from the lateral one third of the distal tibia. The graft was appropriately contoured such that it would smoothly align with the natural arc of the glenoid when aligned flush to the articular surface. Like the Latarjet reconstruction, the graft was affixed to the glenoid using two 1.6mm Kirschner wires, drilled in non-parallel fashion. A reduction clamp (Synthes, West Chester, PA) was also used to provide further compression across the construct and prevent subtle changes in position.

Each specimen was tested after both the Latarjet and the distal tibia bone graft procedures in all three testing positions. Contact pressure, contact area, and peak pressures were recorded three times for each testing condition, with the mean used for data analysis.

Statistical Analysis

Data from the pressure and force measurement software, I-scan (Tekscan, Inc., Boston, MA), were analyzed with descriptive statistics. A repeated one-way analysis of variance with Tukey's Post-Hoc analysis was performed to compare the values between testing conditions. Statistical significance was set to 0.05.

Source of Funding

There were no external sources of funding for this project. All distal tibial allograft specimens were provided by Allosource.

Results

The average anterior-posterior diameter of glenoid specimens was 29.4 ± 3.1 mm (range 24.5-34 mm). Mean glenoid defect width was 9.2±0.75mm (Range 8-10.5mm). The average coracoid thickness (anterior-posterior distance once affixed in the Latarjet-LAT position) before decortication of the inferior surface was 9.5 ± 1.7mm (Range 7-12.8mm). In one specimen, the coracoid was actually 7mm thick, much thinner than its corresponding 30% bone defect which was 9mm wide. After clinically simulated decortication of this coracoid's inferior surface, this difference was further magnified—the resultant thickness was only 6mm.

Post-hoc power analysis demonstrated actual power in contact area testing for all groups was greater than 98%. Actual power for other groups was lower; however, even with a small n, we are confident of the results since to achieve a power of 80% in peak pressures for the 30° abduction group, a sample size of over 662 would be required.

Load testing was successfully performed in all specimens without any occurrence of fracture, loss of fixation, alterations in abduction position, or equipment failure. Tekscan mapping of glenohumeral contact area and contact pressures demonstrated higher pressures and smaller contact areas in the defect group with subsequent edge loading at the defect site. Overall progression of both contact area and contact pressure from the intact to defect to reconstruction stages with the arm in the ABER position is illustrated in **Figure 5**.

Contact Area

After creation of a 30% glenoid defect, measured contact areas for the glenoid face decreased significantly (52-56%, **Table 2**). Glenoid bony reconstruction of the defect with a distal tibial allograft resulted in significantly higher glenohumeral contact area than reconstruction with Latarjet bone blocks in 60° abduction and the ABER position ($p<0.05$).

In regard to the bone loss model, distal tibial allograft reconstruction exhibited significantly higher contact areas than the 30% defect model at all abduction positions. Latarjet reconstruction produced significantly higher contact areas compared to the bone loss model at only the 30° and 60° abduction positions (**Tables 2 and 3, Figure 6a**).

Contact Pressure

With regard to measured contact pressures, creation of a 30% bony defect increased contact pressures by 15% compared to the intact state (**Table 2**). Bony reconstruction with both the Latarjet bone blocks and distal tibial allografts significantly lowered contact pressures compared to the bone loss model at all abduction positions ($p<0.05$, **Table 3**). No significant difference in contact pressures was found between the Latarjet bone block and distal tibia allograft conditions ($p>0.05$, **Figure 6b**).

Peak Force

Distal tibial allograft reconstruction demonstrated significantly lower peak forces than Latarjet reconstruction in the ABER position ($p<0.05$). In the bone loss model, distal tibial

allograft reconstruction produced significantly lower peak forces than the 30% defect model at all abduction positions (**Table 3**). Latarjet reconstruction also exhibited lower peak forces than the defect model at the 30° and 60° abduction positions, but differences in peak force between the defect and Latarjet reconstruction in the ABER position were not statistically significant ($p>0.05$, **Tables 2 and 3, Figure 6c**).

Discussion:

The principal findings of this study demonstrated that glenoid bone reconstruction with distal tibial allografts resulted in significantly higher glenohumeral contact area than reconstruction with Latarjet bone blocks in 60° abduction and the ABER position. Additionally, distal tibial allograft reconstruction also gave rise to significantly lower glenohumeral peak forces than Latarjet reconstruction in the ABER position. Distal tibial allograft reconstruction exhibited significantly higher contact areas and significantly lower contact pressures and peak forces than the 30% defect model at all abduction positions. Latarjet reconstruction also followed this same pattern but differences in contact area and peak forces between the defect model and Latarjet reconstruction in the ABER position were not statistically significant ($p>0.05$). To our knowledge, this is the first study reported in the literature comparing glenohumeral loading mechanics in a clinically relevant anterior instability model, a Latarjet reconstruction model, and a distal tibial osteochondral allograft model.

As noted by Greis and colleagues, a 30% glenoid defect increases glenohumeral anteroinferior contact pressures 300-400%(22), a finding that underscores the need for glenoid reconstruction with adequate bone stock and appropriate graft choice in patients with such injuries. Open glenoid bone augmentation procedures such as the Latarjet, iliac crest bone-grafting, and allograft techniques are currently recommended for any patient with recurrent shoulder instability and greater than 20-25% bone loss. Bone augmentation is necessary in these patients in order to sufficiently reconstitute the glenoid's osseous arc, one of its key static glenohumeral restraints.(1)

In the Latarjet technique, a locally harvested coracoid autograft is transferred such that it can serve as an extension of the glenoid's articular arc. Although the Latarjet technique was originally described in 1954 and has undergone several variations, little consensus exists on optimal graft orientation.(2, 17) In a cadaveric biomechanics study, Ghodadra and colleagues demonstrated that flush positioning of a coracoid graft oriented with its concave undersurface as part of the glenoid arc—the congruent arc modification (Latarjet-INF) as described by De Beer and Burkhart(5)—most optimally restored normal glenohumeral contact pressures and area.(21) Although such a coracoid orientation has been advocated in the literature, patient-specific and intra-operative factors may sometimes make it difficult to achieve adequate fixation while maintaining the Latarjet-INF orientation. In these instances, the more traditional Latarjet-LAT orientation is frequently substituted.

Despite several decades of evolution in surgical techniques employed during Latarjet glenoid reconstruction, shortcomings in patient outcomes still persist. Currently, concerns regarding coracoid transfer techniques include a non-anatomic repair of glenoid defects, poor reconstitution of the glenoid arc, an extra-articular non-anatomic repair of capsulolabral tissues, and no reconstitution of the chondral surface.(12) Allain and colleagues, in a retrospective review of 58 patients undergoing a Latarjet procedure, found that at an average follow-up time of 14.3 years, more than half of these shoulders had glenohumeral arthritis, most of which (twenty-five) were characterized as grade 1 changes.(27) Other authors investigating outcomes after coracoid transfer procedures have noted comparable findings.(15, 19, 20) It is hypothesized that the high rate of glenohumeral degenerative changes in this cohort is multifactorial. Certainly, a high degree of chondral injury occurs preoperatively in this group both at the time of initial dislocation but also during subsequent recurrent instability events. However, the results of this study also suggest that intra-articular peak forces may not completely normalize after a coracoid transfer procedure. In fact, in the ABER position, glenohumeral peak forces after Latarjet reconstruction may be more similar to the defect state than an intact glenoid. Such imperfections in articulation could surely further propogate chondral injury and elevate joint reactive forces, particularly if joint mechanics are also altered.

Use of distal tibial osteochondral allograft for reconstitution of glenoid bone defects is a novel technique that capitalizes on the reality that fresh distal tibial allograft, widely available in tissue banks, contains a robust cartilaginous surface that is highly congruent with the area of glenoid bone loss.(12) Allograft tissue offers all the benefits of avoiding donor-site morbidity that is frequently associated with coracoid transfer or autograft procedures. When comparisons with glenoid allografts are made, distal tibial allograft is more readily available because the glenoid, a more centrally located structure in the body, is more subject to graft contamination during harvesting. Initial data have shown that the lateral aspect of the distal tibia has a radius of curvature that is quite similar to the glenoid's osseous arc as well as the humeral head. Any subtle differences in curvature can usually be tailored to a precise fit intra-operatively.(12) Moreover, because this tissue source contains dense weight-bearing corticocancellous bone, superb screw fixation can be observed and the potential for excellent host-graft incorporation exists. Finally, it should be noted that distal tibial allografts allow reconstitution of actual bone loss as opposed to a limited amount defined by coracoid dimensions. As noted in this study, coracoid thickness was sometimes smaller than the actual amount of bone loss, particularly after clinically simulated decortication of the inferior surface. In these instances, a coracoid graft would not be able to fully restore the glenoid's osseous arc. Bueno and authors, in an anatomic study of 31 scapulae, noted that anteroposterior coracoid thickness (thickness of an unaltered coracoid graft in Latarjet-LAT graft position) was at times only 25% of the corresponding glenoid's width, a finding that complicates glenoid bone restitution in cases with severe defects.(28) Ljungquist and colleauges, in an anatomic study of 100 scapulae, also noted similar findings and concluded that allograft is generally preferred over coracoid for larger bone defects,

especially when coracoid graft is proportionately smaller and used in the standard Latarjet-LAT position.(29)

In summary, this is the first biomechanical cadaveric study to compare glenohumeral loading mechanics in a clinically relevant anterior instability model, a Latarjet reconstruction model, and a distal tibial osteochondral allograft model. In addition to the study design, various strengths of this study include a standardized testing protocol, randomization to different testing arms, and glenoid reconstruction in clinically relevant configurations and patterns. Nonetheless, the study is not without some inherent limitations. Cadaveric tissue does not allow for in vivo evaluation of glenohumeral mechanics, osseous healing, subjective outcomes, or alterations in dynamic constraints in glenohumeral stability following glenoid reconstruction with either the Latarjet technique or distal tibia allograft. Such information would have been useful, particularly since coracoid transfer techniques have the added benefit of creating a sling with the conjoined tendon in order to oppose anterior humeral translation in the ABER position. Cadaveric bone and cartilage is also softer and more predisposed to deformation with excessive load testing. To counteract this limitation, the order in which specimens underwent either a Latarjet or distal tibial glenoid reconstruction (with subsequent testing) was randomized. Tissues were also meticulously kept moist with 0.9% normal saline throughout testing. Finally, it is important to note that our study did not evaluate loading patterns in the congruent arc modification of the Latarjet technique (Latarjet-INF position). Although placing the coracoid in this orientation has been reported to have an improved contact pressure profile than the Latarjet-LAT position, difficulties with fixation have not allowed this technique to be widely utilized in our clinical practice.

Conclusions:

Principles of surgical management in patients with glenoid bone loss are guided by the extent of osseous injury, the surgeon's personal experience with specific reconstructive techniques, and patient specific factors such as work and athletic demands.(1) Open glenoid bone augmentation procedures such as the Latarjet, iliac crest bone-grafting, and allograft techniques are currently recommended for any patient with recurrent shoulder instability and greater than 20-25% bone loss. The principal findings of this study indicate that glenoid bone reconstruction with distal tibial osteochondral allograft results in significantly improved glenohumeral contact area than reconstruction with a Latarjet bone block in 60° abduction and the ABER position. Additionally, distal tibial allograft reconstruction also results in significantly lower glenohumeral peak forces than Latarjet reconstruction in the ABER position. Further studies are needed to delineate the effects this improved articulation may have on post-operative outcomes following glenoid reconstruction.

Tables

Table 1. Demographics of shoulder specimens. (n=8 specimens).

Demographic Category	*Characteristic*
Left/right	5 right 3 left
Age	48.6 ± 6.9 years Range (38-58 years)
Gender	Male - 3 (37.5%) Female - 5 (62.5%)
Cause of death	Myocardial Infarction - 1 (12.5%) Pneumonia – 2 (25%) Hypertensive cardiovascular disease – 1 (12.5%) Metastatic skin cancer – 1 (12.5%) Melanoma – 2 (25%) Lung cancer – 1 (12.5%)

Table 2. Normalization of glenohumeral contact area, contact pressure, and peak force after creation of a 30% glenoid defect, Latarjet reconstruction, and glenoid reconstruction with a distal tibial osteochondral allograft. Notable values are in bold.

	30 deg (% of intact)			60 deg (% of intact)			ABER (% of intact)		
	Defect	*Latarjet*	*Distal Tibia*	*Defect*	*Latarjet*	*Distal Tibia*	*Defect*	*Latarjet*	*Distal Tibia*
Contact area	56.14	74.74	88.04	52.09	73.62	**90.4***	52.84	**71.27†**	**101.4***
Contact Pressure	115.4	106.97	102.33	116.13	104.61	100.91	115.09	104.48	101.3
Peak Force	107.63	101.47	101.28	113.62	108.17	105.28	113.49	**109.49†**	**100.4***

*Comparison between distal tibia and Latarjet statistically significant ($p < 0.05$)
†Comparison between defect and Latarjet not statistically significant ($p > 0.05$)

Table 3. Results of 1 way ANOVA with Tukey's Post-Hoc test. Note that distal tibial glenoid reconstruction provided significantly increased glenohumeral contact area as compared with the Latarjet reconstruction at 60° abduction and at 60° abduction/90° external rotation (ABER position). Distal tibial glenoid reconstruction also resulted in significantly less glenohumeral peak forces in the ABER position as compared with the Latarjet model. The distal tibial glenoid reconstruction was significantly superior to the defect model in all testing conditions. The Latarjet reconstruction model was also significantly superior to the defect model in all positions except in ABER.

1 Way ANOVA with Tukey's Post-Hoc Test			
	Defect vs Latarjet	***Defect vs Tibia***	***Tibia vs Latarjet***
30° Contact Area	$p < 0.05$	$p < 0.05$	No significance
60° Contact Area	$p < 0.05$	$p < 0.05$	**$p < 0.05$**
60-90° Contact Area	**No significance**	$p < 0.05$	**$p < 0.05$**
30° Contact Pressure	$p < 0.05$	$p < 0.05$	No significance
60° Contact Pressure	$p < 0.05$	$p < 0.05$	No significance
60-90° Contact Pressure	$p < 0.05$	$p < 0.05$	No significance
30° Peak Force	$p < 0.05$	$p < 0.05$	No significance
60° Peak Force	$p < 0.05$	$p < 0.05$	No significance
60-90° Peak Force	**No significance**	$p < 0.05$	**$p < 0.05$**

Figures

Figure 1. Glenoids from 8 fresh-frozen human cadaver shoulders (5 right shoulders and 3 left shoulders from donors with a mean age of 49 [range, 38-58 years] at the time of death) were dissected free of all soft tissues except the labrum.

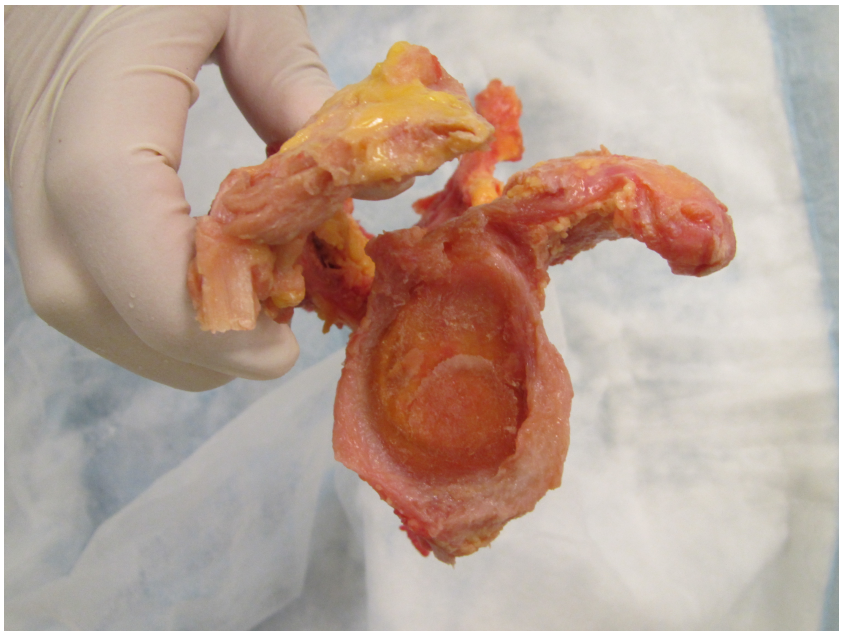

Figure 2. The testing sequence included four conditions: (A) intact glenoid, (B) glenoid with 30% anterior bone defect of glenoid surface area from two o'clock to six o'clock, (C) 30% glenoid defect with a Latarjet bone block placed flush with the lateral surface of the coracoid becoming the glenoid face (Latarjet-LAT), (D) 30% glenoid defect with a distal tibia bone block placed flush.

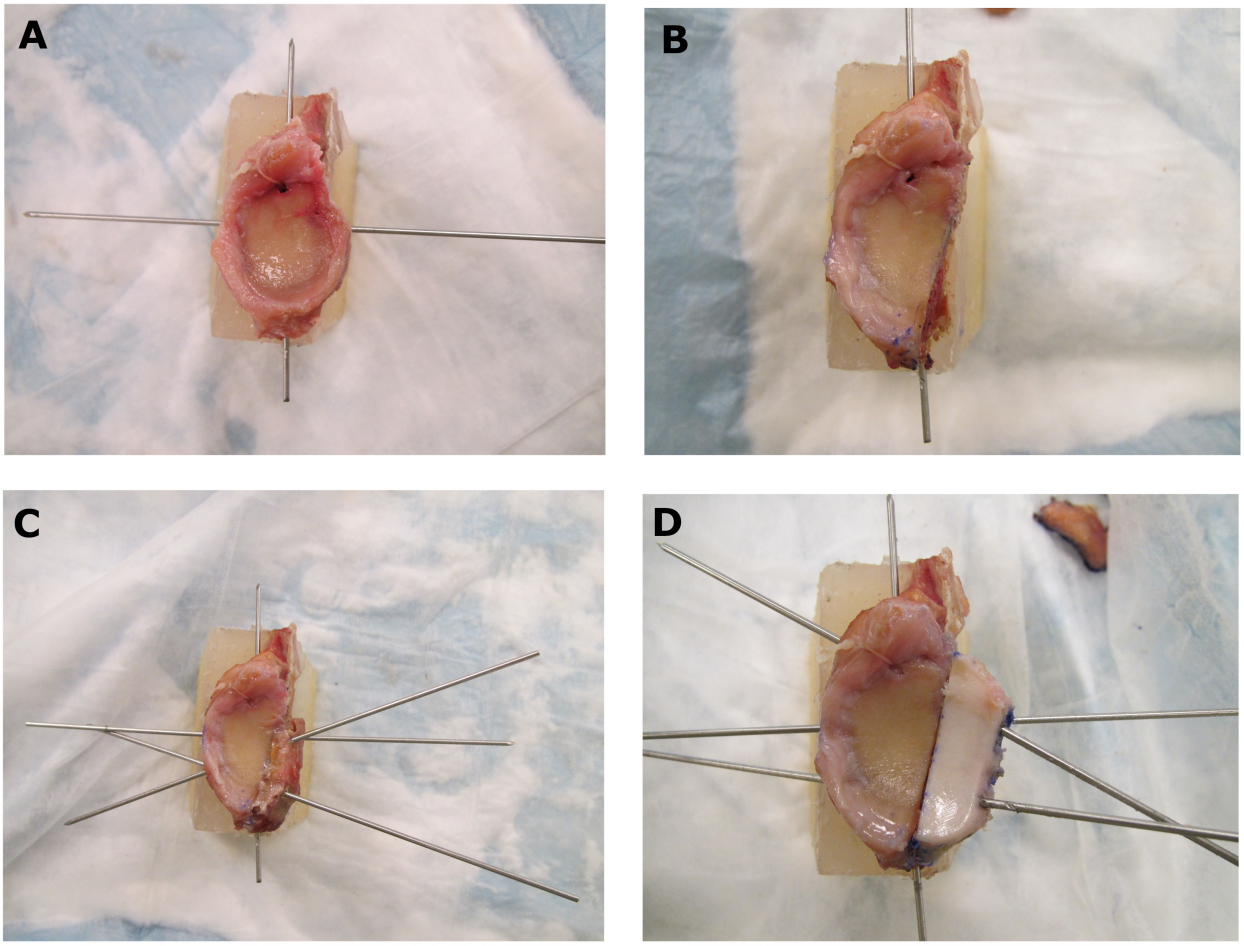

Figure 3. An osteotomy simulating at least 30% bone loss was performed based on a modification of the glenoid bone loss quantification techniques put forth by Sugaya(11) and Burkhart(23). As noted in the literature, the amount of glenoid bone loss can be calculated by using the formula *Defect size = (B-A)/2B x 100%*, where *B* is the radius of the glenoid's true fit circle and *A* is the distance from the circle center to the edge of the defect. Because defect size was known (in our case, 30%), the formula was rearranged to algebraically solve for *A*. For each specimen, the anterior-posterior diameter of the glenoid (two times the radius, *B*) was precisely measured using digital calipers. The distance from the circle center to the osteotomy site (*A*) was then solved for algebraically. A true-fit circular template was then created with the same diameter as the glenoid specimen and was cut *A* millimeters from the center in order to replicate the 30% osteotomy site. The template was then applied to the glenoid and oriented such that a clinically relevant osteotomy, one parallel to the long axis of the glenoid, could be created.

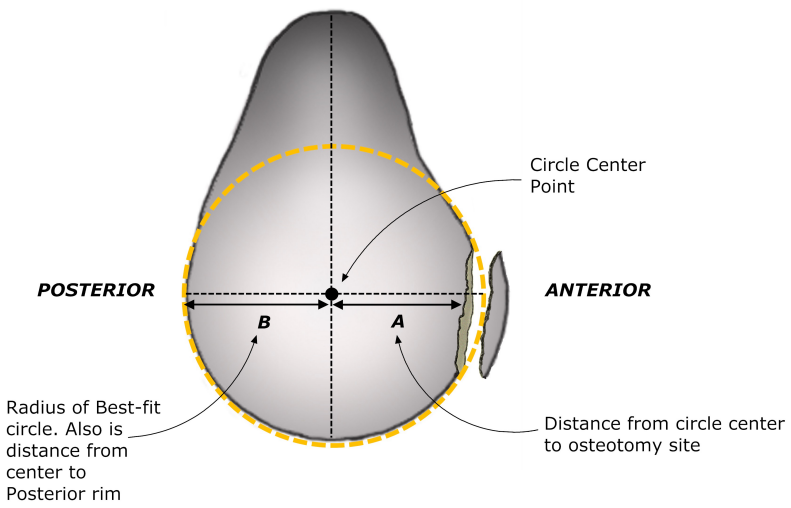

$$\text{Percent Bone Loss} = \frac{(B-A)}{2\times B} \times 100\%$$

Figure 4. Saw bone model of glenoid illustrating how the Latarjet-LAT position was achieved. The coracoid graft was rotated 90° such that the lateral aspect of the coracoid reconstituted the glenoid face and the inferior surface of the coracoid was apposed to the glenoid neck.(16, 26) Additionally, the graft was positioned so that the lateral surface was flush with the glenoid face.(21)

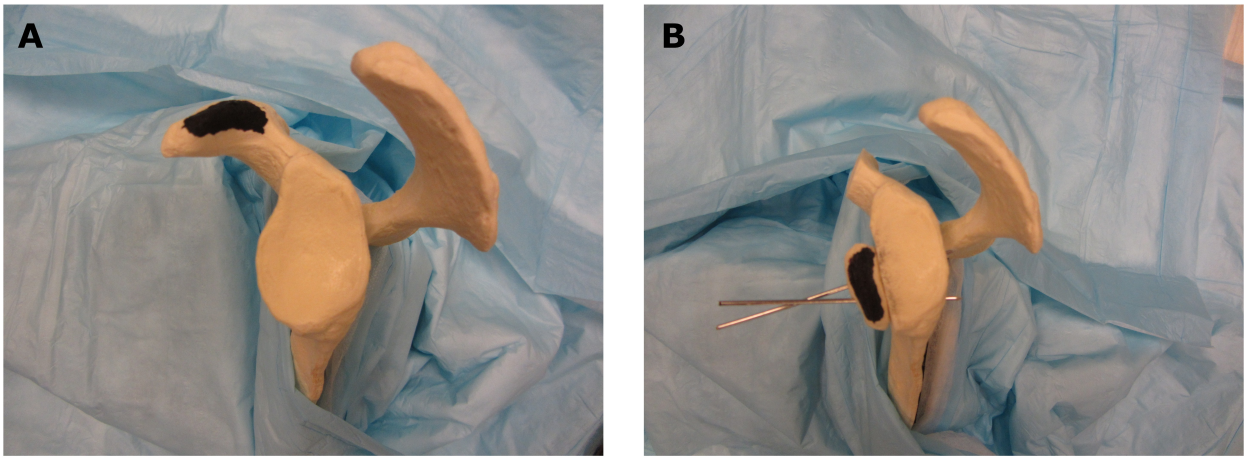

Figure 5. Glenohumeral contact pressure map with the arm in 60 degrees abduction and 90 degrees external rotation (ABER position). Higher pressures are signified by yellow and orange, lower pressures by blue and green (see scale). (A) Intact glenoid; (B) glenoid with 30% anterior bone defect (right side of screen); (C) glenoid after Latarjet bone graft procedure; (D) glenoid after bone reconstruction with distal tibial allograft.

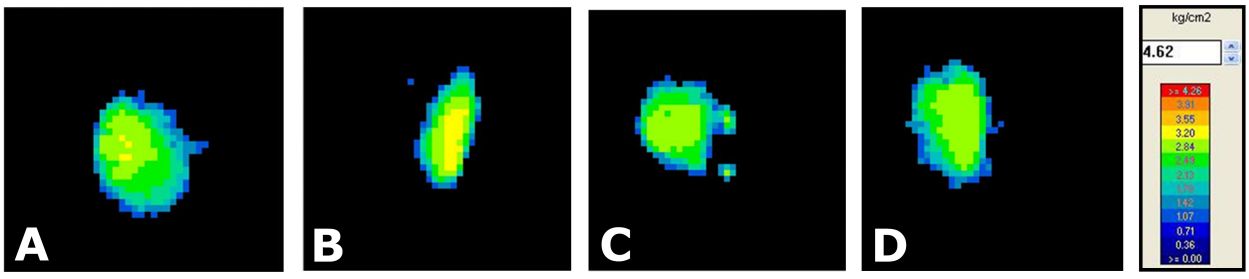

Figure 6. Average glenohumeral contact area (A), contact pressure (B), and peak force (C) in all four states at all three humerus positions.

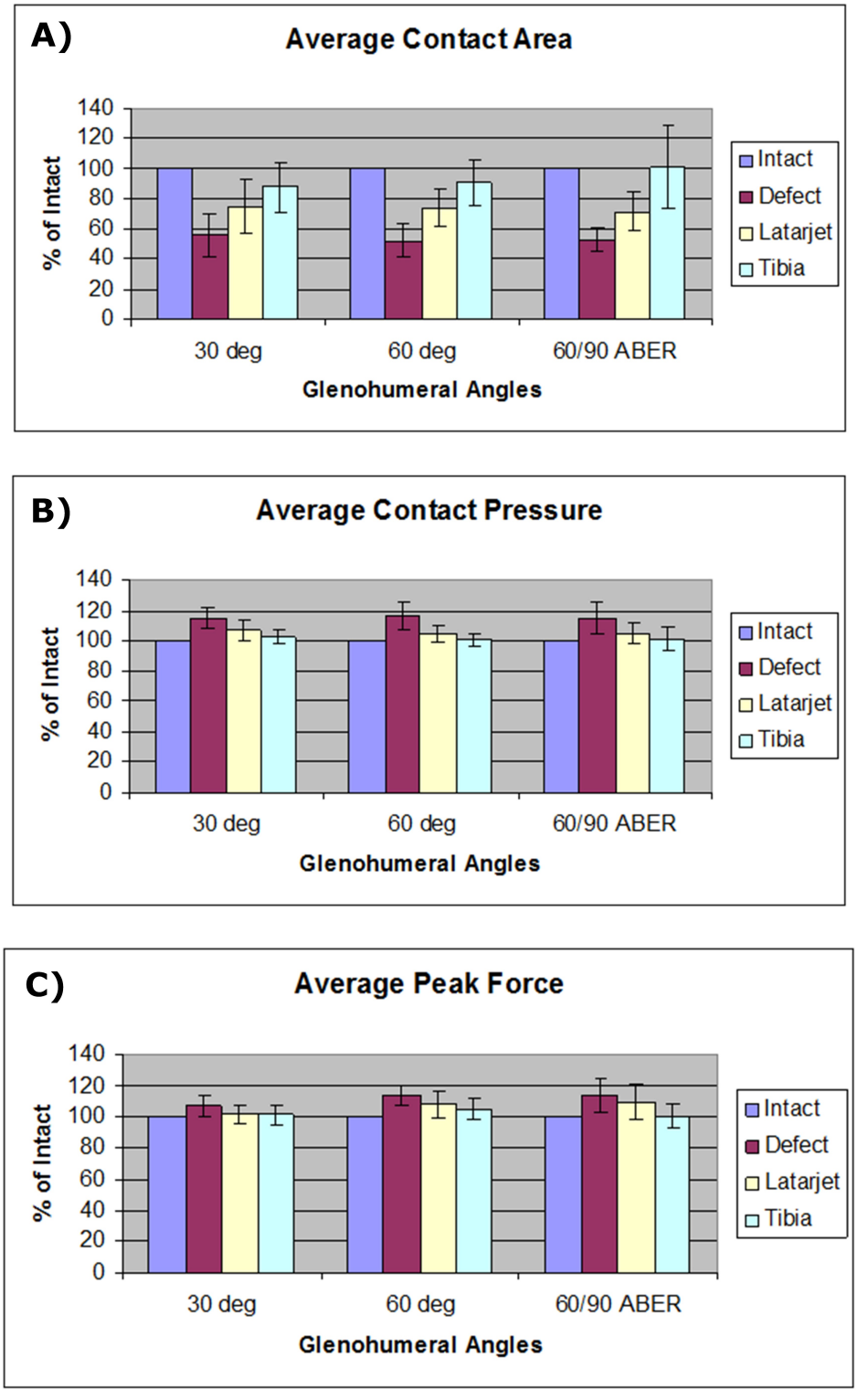

References

1. Provencher MT, Bhatia S, Ghodadra NS, Grumet RC, Bach BR, Jr., Dewing CB, et al. Recurrent shoulder instability: current concepts for evaluation and management of glenoid bone loss. J Bone Joint Surg Am. 2010 Dec;92 Suppl 2:133-51.
2. Piasecki DP, Verma NN, Romeo AA, Levine WN, Bach BR, Jr., Provencher MT. Glenoid bone deficiency in recurrent anterior shoulder instability: diagnosis and management. J Am Acad Orthop Surg. 2009 Aug;17(8):482-93.
3. Howell SM, Galinat BJ. The glenoid-labral socket. A constrained articular surface. Clin Orthop Relat Res. 1989 Jun(243):122-5.
4. Mologne TS, Provencher MT, Menzel KA, Vachon TA, Dewing CB. Arthroscopic stabilization in patients with an inverted pear glenoid: results in patients with bone loss of the anterior glenoid. Am J Sports Med. 2007 Aug;35(8):1276-83.
5. Burkhart SS, De Beer JF. Traumatic glenohumeral bone defects and their relationship to failure of arthroscopic Bankart repairs: significance of the inverted-pear glenoid and the humeral engaging Hill-Sachs lesion. Arthroscopy. 2000 Oct;16(7):677-94.
6. Montgomery WH, Jr., Wahl M, Hettrich C, Itoi E, Lippitt SB, Matsen FA, 3rd. Anteroinferior bone-grafting can restore stability in osseous glenoid defects. J Bone Joint Surg Am. 2005 Sep;87(9):1972-7.
7. Warner JJ, Gill TJ, O'Hollerhan J D, Pathare N, Millett PJ. Anatomical glenoid reconstruction for recurrent anterior glenohumeral instability with glenoid deficiency using an autogenous tricortical iliac crest bone graft. Am J Sports Med. 2006 Feb;34(2):205-12.
8. Boileau P, Bicknell RT, El Fegoun AB, Chuinard C. Arthroscopic Bristow procedure for anterior instability in shoulders with a stretched or deficient capsule: the "belt-and-suspenders" operative technique and preliminary results. Arthroscopy. 2007 Jun;23(6):593-601.
9. Kim SH, Ha KI, Kim YM. Arthroscopic revision Bankart repair: a prospective outcome study. Arthroscopy. 2002 May-Jun;18(5):469-82.
10. Lafosse L, Lejeune E, Bouchard A, Kakuda C, Gobezie R, Kochhar T. The arthroscopic Latarjet procedure for the treatment of anterior shoulder instability. Arthroscopy. 2007 Nov;23(11):1242 e1-5.
11. Sugaya H, Kon Y, Tsuchiya A. Arthroscopic repair of glenoid fractures using suture anchors. Arthroscopy. 2005 May;21(5):635.
12. Provencher MT, Ghodadra N, LeClere L, Solomon DJ, Romeo AA. Anatomic osteochondral glenoid reconstruction for recurrent glenohumeral instability with glenoid deficiency using a distal tibia allograft. Arthroscopy. 2009 Apr;25(4):446-52.
13. Bigliani LU, Newton PM, Steinmann SP, Connor PM, McLlveen SJ. Glenoid rim lesions associated with recurrent anterior dislocation of the shoulder. Am J Sports Med. 1998 Jan-Feb;26(1):41-5.

14. Burkhart SS, De Beer JF, Barth JR, Cresswell T, Roberts C, Richards DP. Results of modified Latarjet reconstruction in patients with anteroinferior instability and significant bone loss. Arthroscopy. 2007 Oct;23(10):1033-41.
15. Hovelius LK, Sandstrom BC, Rosmark DL, Saebo M, Sundgren KH, Malmqvist BG. Long-term results with the Bankart and Bristow-Latarjet procedures: recurrent shoulder instability and arthropathy. J Shoulder Elbow Surg. 2001 Sep-Oct;10(5):445-52.
16. Salvi AE, Paladini P, Campi F, Porcellini G. The Bristow-Latarjet method in the treatment of shoulder instability that cannot be resolved by arthroscopy. A review of the literature and technical-surgical aspects. Chir Organi Mov. 2005 Oct-Dec;90(4):353-64.
17. Latarjet M. [Treatment of recurrent dislocation of the shoulder]. Lyon Chir. 1954 Nov-Dec;49(8):994-7.
18. Hovelius L, Sandstrom B, Sundgren K, Saebo M. One hundred eighteen Bristow-Latarjet repairs for recurrent anterior dislocation of the shoulder prospectively followed for fifteen years: study I--clinical results. J Shoulder Elbow Surg. 2004 Sep-Oct;13(5):509-16.
19. Oster A. Recurrent anterior dislocation of the shoulder treated by the Eden-Hybinette operation. Follow-up on 78 cases. Acta Orthop Scand. 1969;40(1):43-52.
20. Hindmarsh J, Lindberg A. Eden-Hybbinette's operation for recurrent dislocation of the humero-scapular joint. Acta Orthop Scand. 1967;38(4):459-78.
21. Ghodadra N, Gupta A, Romeo AA, Bach BR, Jr., Verma N, Shewman E, et al. Normalization of glenohumeral articular contact pressures after Latarjet or iliac crest bone-grafting. J Bone Joint Surg Am. 2010 Jun;92(6):1478-89.
22. Greis PE, Scuderi MG, Mohr A, Bachus KN, Burks RT. Glenohumeral articular contact areas and pressures following labral and osseous injury to the anteroinferior quadrant of the glenoid. J Shoulder Elbow Surg. 2002 Sep-Oct;11(5):442-51.
23. Burkhart SS, Debeer JF, Tehrany AM, Parten PM. Quantifying glenoid bone loss arthroscopically in shoulder instability. Arthroscopy. 2002 May-Jun;18(5):488-91.
24. Saito H, Itoi E, Sugaya H, Minagawa H, Yamamoto N, Tuoheti Y. Location of the glenoid defect in shoulders with recurrent anterior dislocation. Am J Sports Med. 2005 Jun;33(6):889-93.
25. Provencher MT, Detterline AJ, Ghodadra N, Romeo AA, Bach BR, Jr., Cole BJ, et al. Measurement of glenoid bone loss: a comparison of measurement error between 45 degrees and 0 degrees bone loss models and with different posterior arthroscopy portal locations. Am J Sports Med. 2008 Jun;36(6):1132-8.
26. Schroder DT, Provencher MT, Mologne TS, Muldoon MP, Cox JS. The modified Bristow procedure for anterior shoulder instability: 26-year outcomes in Naval Academy midshipmen. Am J Sports Med. 2006 May;34(5):778-86.
27. Allain J, Goutallier D, Glorion C. Long-term results of the Latarjet procedure for the treatment of anterior instability of the shoulder. J Bone Joint Surg Am. 1998 Jun;80(6):841-52.

28. Bueno RS, Ikemoto RY, Nascimento LG, Almeida LH, Strose E, Murachovsky J. Correlation of Coracoid Thickness and Glenoid Width: An Anatomic Morphometric Analysis. Am J Sports Med. 2012 May 4.
29. Ljungquist KL, Butler RB, Griesser MJ, Bishop JY. Prediction of coracoid thickness using a glenoid width-based model: implications for bone reconstruction procedures in chronic anterior shoulder instability. J Shoulder Elbow Surg. 2012 Jan 2.